Proceedings of the 7th International Conference on Mechanics and Materials in Design
Albufeira/Portugal 11-15 June 2017. Editors J.F. Silva Gomes and S.A. Meguid.
Publ. INEGI/FEUP (2017)

PAPER REF: 6569

STRENGTH ANALYSIS OF LASER BEAM WELDED STEEL - ALUMINIUM JOINTS FOR MARITIME LIGHT WEIGHT APPLICATIONS

Benjamin Möller[1(*)], Rainer Wagener[1], Tobias Melz[1], Rabi Lahdo[2], André Springer[2], Stefan Kaierle[2], Ludger Overmeyer[2]

[1]Fraunhofer Institute for Structural Durability and System Reliability LBF, Darmstadt, Germany
[2]Laser Zentrum Hannover e.V., Hannover, Germany
[(*)]*Email:* benjamin.moeller@lbf.fraunhofer.de

ABSTRACT

The application of a laser beam welding process to join steel to aluminium using a high-power laser is demonstrated to provide a joining process for semi-manufactured steel-aluminium products for the maritime industry. On the basis of lap joints made of S355 steel (t = 5 mm) and the aluminium alloy EN AW-6082 T651 (t = 8 mm), the feasibility of joining dissimilar materials is shown. To date, a combination of steel and aluminium is well known to have a low weldability due to the differing physiochemical properties of the two materials and the formation of intermetallic phases. The weld seam quality and strength greatly depends on the amount of intermetallic phases within the joint and the local weld geometry, so that different process parameters are investigated within the welding process development. Quasi-static investigations on lap joints and adapter specimens, with up to six weld seams, show an increase of the tensile shear strength for optimised parameters and for an increased number of weld seams. The dependency of the quality of the weld on the major geometrical parameters, weld width and penetration depth, is moreover shown by the fatigue strength of lap joints. Promising fatigue test results on adapter specimens emphasise the potential for applying steel-aluminium laser welds in ship design in the future.

Keywords: fatigue, lap joint, high-power laser welding, steel-aluminium dissimilar joint.

INTRODUCTION

The Energy Efficiency Design Index (EEDI) has been introduced in order to reduce the CO_2 footprint and, hence, the fuel consumption in shipping (ICCT, 2011). An increased environmental consciousness in ship building, as well as in the automotive industry, has advanced lightweight design. In the course of decreasing fuel consumption and decreasing the total shipping weight, lightweight construction materials, such as aluminium, are used and have to be joined in hybrid material combinations. Therefore, costly explosive welding is used to join steel to aluminium in the field of yacht design. Fig. 1 shows a designed explosive welded adapter (Buijs, 2004) and the application area within ship design (FSW-Ship project, 2013). An overview of the many mechanical and thermal technologies for welding steel to aluminium is given by Lahdo *et al.* (Lahdo *et al.*, 2016). The aim of recent research has been to substitute the planar joined adapter, manufactured by the costly and time consuming explosive welding technology.

However, in thermal joining processes (e.g. laser beam welding) of dissimilar materials, differing physiochemical properties, characterised by different melting points, thermal conductivities and thermal expansion coefficients, as well as the formation of intermetallic compounds (brittleness), due to limited solubility, have to be considered (Klock and Schroer, 1977; Kreimeyer *et al.*, 2004). As a result of an increased hardness of approximately 1000 HV and a low ductility, the existence of intermetallic phases with high aluminium content, particularly Fe_2Al_5 und $FeAl_3$, in the weld seam weakens the welded joint (Kallage, 2013). Therefore, the material combination of steel and aluminium has been well known to date for exhibiting a low weldability.

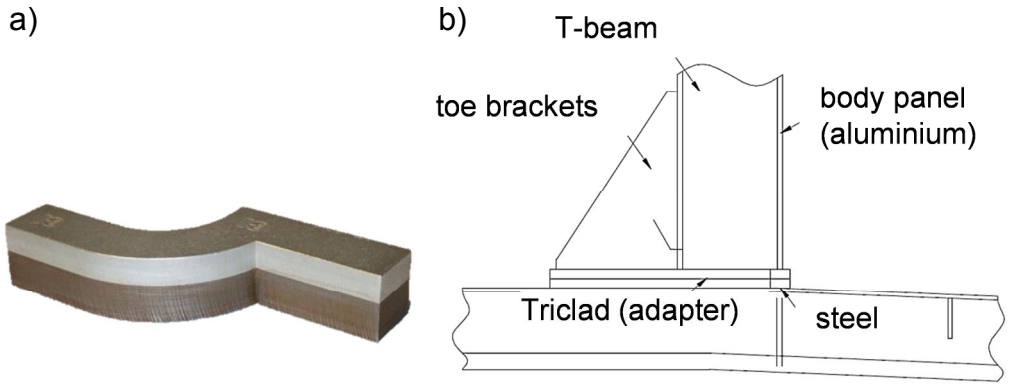

Fig. 1 - Explosive welded adapter (Buijs, 2004) (a) and a typical application of steel-aluminium joints in ship design (FSW-Ship project, 2013) (b)

EXPERIMENTAL PROCEDURE

The feasibility of a joining process for dissimilar materials, such as steel and aluminium, for maritime applications will be presented using the high-power laser welding system TruDisk 16.002 with a maximum laser power of 16 kW (Trumpf Laser- und Systemtechnik GmbH). A focal length of 300 mm and a line of collimation with a length of 200 mm were used, so that a theoretical spot diameter of 0.3 mm resulted when considering a fibre diameter of 0.2 mm. The development of an adequate one-sided welding process was carried out on dissimilar lap joints made of the aluminium alloy EN AW-6082 T651 (t = 8 mm) and S355 steel (t = 5 mm) with the mechanical properties defined in Table 1. For the determination of the influence of the fusion zone with respect to the formation of intermetallic phases, the weld width and penetration depth as well as existing cracks were investigated in weld trails with a constant laser power of 6 kW and a variation in welding speed. The welding trials were carried out using spot diameters of 0.6 mm and 1.2 mm (corresponding to a defocusing of Δz = -5.0 mm and Δz = -12.5 mm).

Table 1 - Mechanical properties of applied materials and the ref. material EN AW-5083 H111

Material	Yield strength [MPa]	Tensile strength [MPa]
S355 (t = 5 mm)	456	556
EN AW-6082 T651 (t = 8 mm)	303	325
EN AW-5083 H111 (t = 8 mm, reference material)	145	287

In order to characterise the mechanical properties of the joint, specimens of 25 mm width were manufactured from the welded sheets by water cutting. A one-sided lap joint with a

single weld seam is shown in Fig. 2 (a). In addition to a single weld seam, the influence of the number of welds was investigated using specimens with multiple weld seams, cf. Fig. 2 (b). On the basis of multiple lap joints, an adapter specimen made of S355 and EN AW-6082 T651 corresponding to Fig. 2 (c) has been developed. The final aim of the research work was to design an adapter, which can be manufactured as a semi-finished product and integrated into the production process of a ship. This adapter will be applied as a link between the hull, made of shipbuilding steel, and the superstructure, made of an aluminium alloy, e.g. EN AW-5083 H111, whose mechanical properties have been added to Table 1.

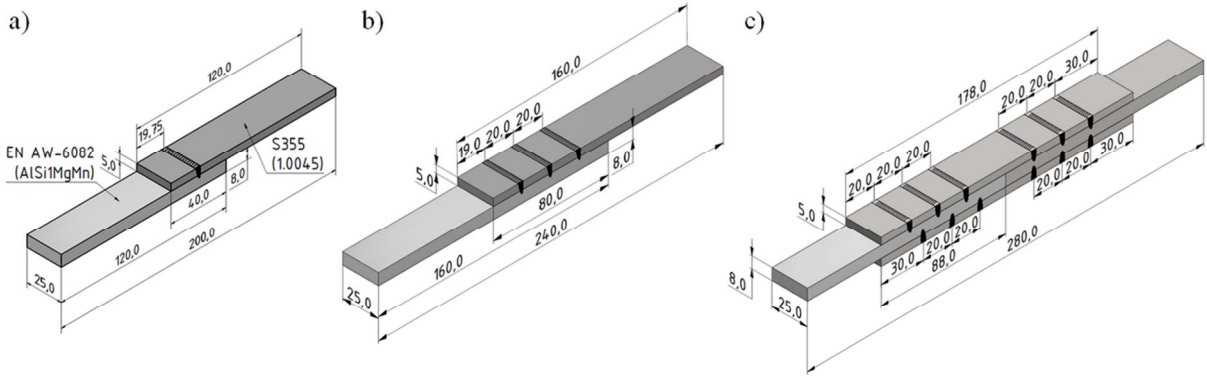

Fig. 2 - Lap joint with a single weld seam (a), a triple weld seam (b) and an adapter specimen with six weld seams (c)

The assessment of laser beam welded steel-aluminium joints consisted of three stages, as shown in Fig. 3. Firstly, geometrical parameters (weld width between the steel and aluminium sheet, penetration depth of the weld into the aluminium alloy as well as crack length of the fusion zone) of the welds were evaluated. Secondly, the quasi-static mechanical properties of lap joints and adapter specimens, produced using promising process parameters, were determined and, thirdly, fatigue strength was investigated by fatigue testing for two parameter sets.

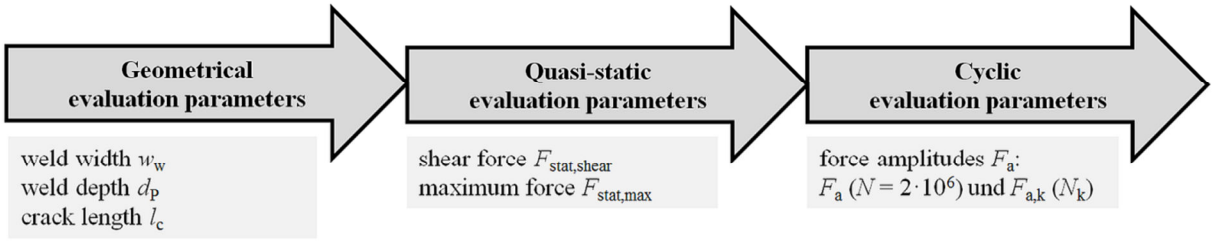

Fig. 3 - Assessment procedure for steel-aluminium laser welded joints

RESULTS

Weld geometry and crack length resulting from analysis of the micro-section

In order to determine the influence of the energy per unit length on the weld seam geometry, the weld width w_w, the penetration depth d_p, and the crack length $l_{c,}$, measured in micro-sections of the steel-aluminium lap joint, were taken. These parameters were investigated using a light microscope. The measured crack length was the summation of all cracks within the weld-in area of the aluminium alloy, as shown in Fig. 4(2). The measured values and the micro-sections, presented in Fig. 4, show the interaction of the energy per unit length for bothof the spot diameters used, $d_s = 0.6$ mm (top) and $d_s = 1.2$ mm (bottom). For both spot diameters, the weld width and the penetration depth increased with increasing energy per unit

length. An average width weld between 0.7 mm and 0.9 mm and an average penetration depth between 0.5 mm and 1.0 mm were found when using a spot diameter of 0.6 mm. In contrast to the smaller spot diameter of 0.6 mm, an average weld width between 1.3 mm and 1.7 mm and an average penetration depth between 1.2 mm and 2.7 mm were determined when using a spot diameter of 1.2 mm. However, there was a high degree of scatter of the measured values, regardless of spot diameter.

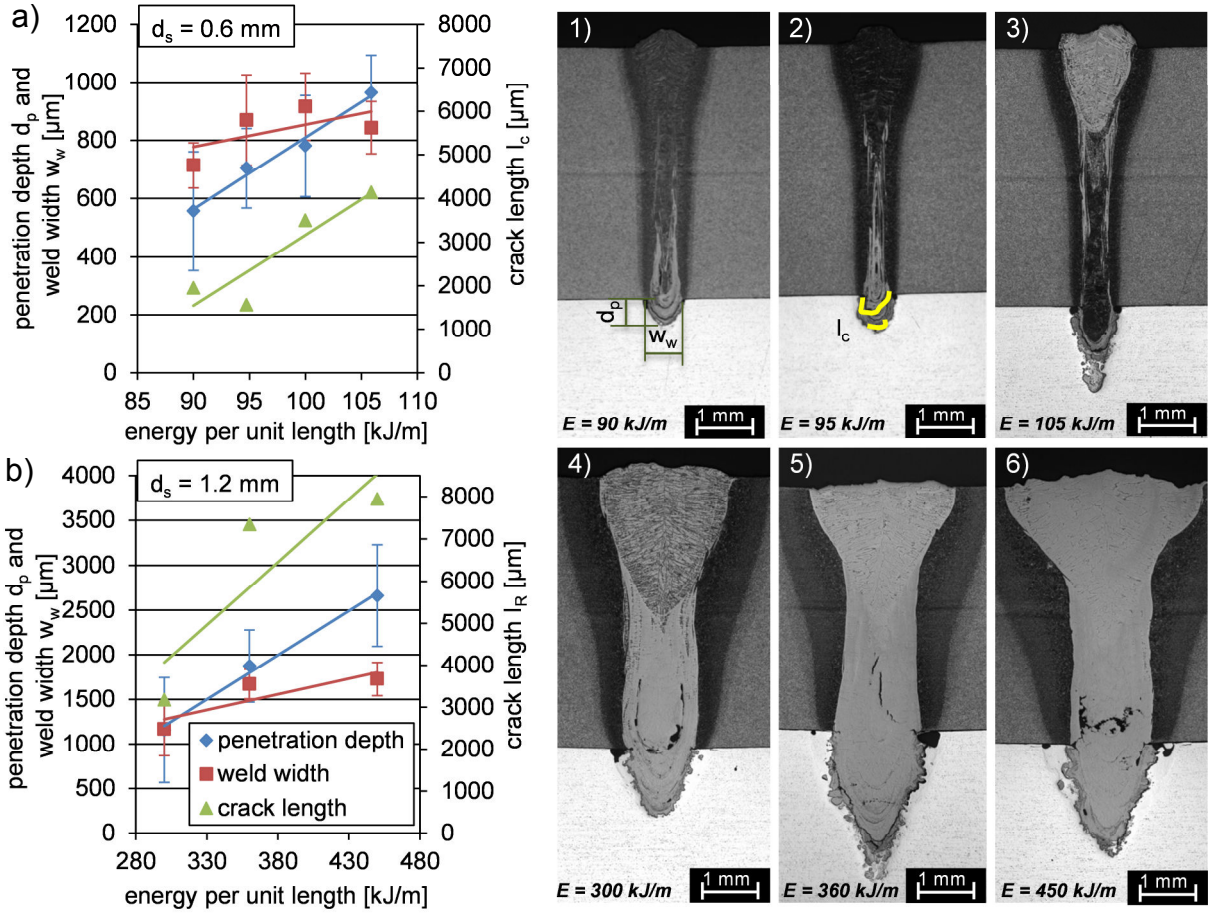

Fig. 4 - Penetration depth, weld width and crack length as a function of the energy per unit length using a spot diameter d_s of 0.6 mm (a) with cross-sections (1-3) and d_s 1.2 mm (b) with cross-sections (4-6)

The crack length increased with an increasing penetration depth, as a result of a higher energy per unit length. The increased crack length can be explained by the fact that higher aluminium content in the weld metal tends to form a higher proportion of hard and brittle intermetallic compounds. In particular, the different coefficients of thermal expansion of steel material and aluminium alloy, combined with brittleness, create cracks during the solidification.

In addition, the measurement of the weld width and the penetration depth of all weld seams was performed, not only based on micro-sections, but also using a sensing device for all lap specimens. The ratio between weld width and penetration depth w_w/t_p can be used as a parameter that is related to the fatigue strength. The parameters vary strongly within each testing series and, even, within a part of the weld seam. In order to improve the reproducibility of the weld seam geometry, the penetration depth must be adjusted by a control unit.

Evaluation under quasi-static loading

Tensile shear tests were carried out to determine the influence of the energy per unit length on the shear force for the two different spot diameters of 0.6 mm and 1.2 mm.

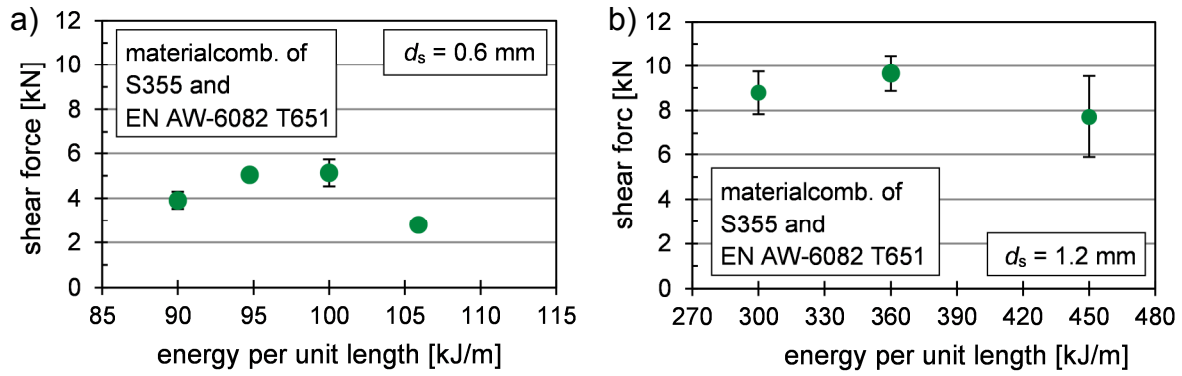

Fig. 5 - Results of the tensile shear tests using spot diameters of d_s = 0.6 mm (a) and d_s = 1.2 mm (b)

In Fig. , the results of the tensile shear tests (shear forces) for the spot diameters of 0.6 mm, Fig. (a), and of 1.2 mm, Fig. (b), are shown. The convex course of the shear force is similar for both spot diameters, so that a maximum can be found with an increasing energy per unit length, after which there is a decrease, despite an increasing weld width, as a result of an even higher energy per unit length. For the latter case, the negative influence of increasing crack length on the shear force is higher compared to the increase in weld width. Especially, transversal cracks lead to a premature failure of the weld seam, when a high energy per unit length and, hence, penetration depth are applied. However, using a spot diameter of 0.6 mm and an energy per unit length of 95 kJ/m, a shear force of approximately 5 kN is achieved. With a spot diameter of 1.2 mm, a higher maximum shear force of 9.7 kN is found using an energy per unit length of 360 kJ/m (welding speed of 1.0 m/min).

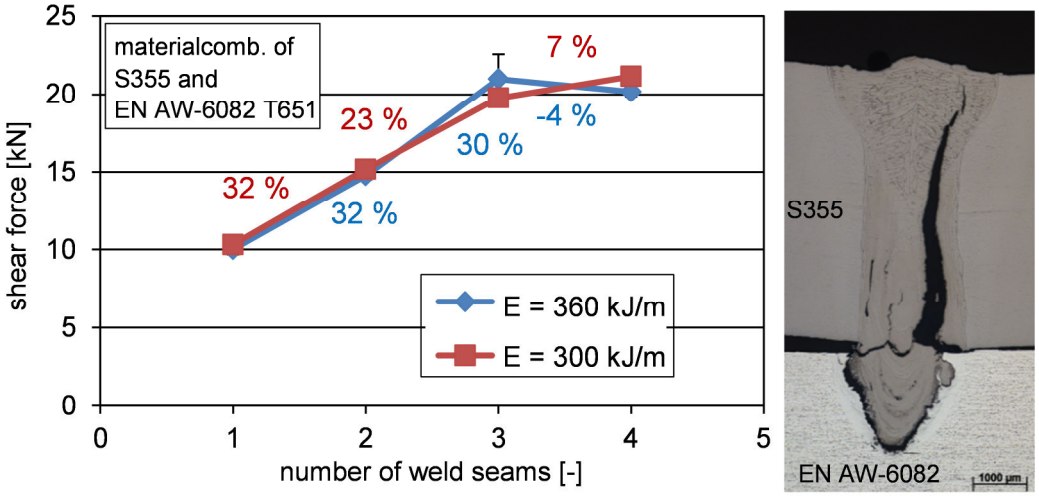

Fig. 6 -Results of the tensile shear tests for varying numbers of weld seams using a constant energy per unit length of 300 kJ/m and of 360 kJ/m

In order to investigate the influence of the number of weld seams on the shear forces, the number of weld seams was varied from one to four using a spot diameter of 1.2 mm and a constant energy per unit length of $E = 300$ kJ/m and $E = 360$ kJ/m, respectively. Fig. 6 shows the results of the tensile shear tests for multiple weld seams. The shear force increased continuously for the welding process with an energy per unit length of 300 kJ/m: around 32 % from one to two weld seams, 23 % from two to three weld seams and 7 % from three to four weld seams. The maximum shear force of 21 kN was reached for four parallel laser weld seams. At an energy per unit length of 360 kJ/m, the maximum shear force was found for three weld seams. In contrast to the results for $E = 300$ kJ/m, the shear force decreases slightly, by 4 %, when increasing the number of weld seams from three to four. This can be explained by a higher distortion resulting from a higher energy per unit length. Therefore, the weld seam is loaded by additional bending stresses induced by clamping into the test rig. In conclusion, three parallel weld seams were chosen for the manufacture of the adapter.

The steel-aluminium adapter was manufactured by a double-side welding of each three weld seams using a spot diameter of 1.2 mm, see Fig. 2(c). A sample (length: 280 mm, width: 25 mm) of the adapter was taken to determine the maximum tensile force under quasi-static loading. Fig. 7 shows the result of the tensile tests, where the penetration depth depends on the energy per unit length and, therefore, determines the static strength of the adapter.

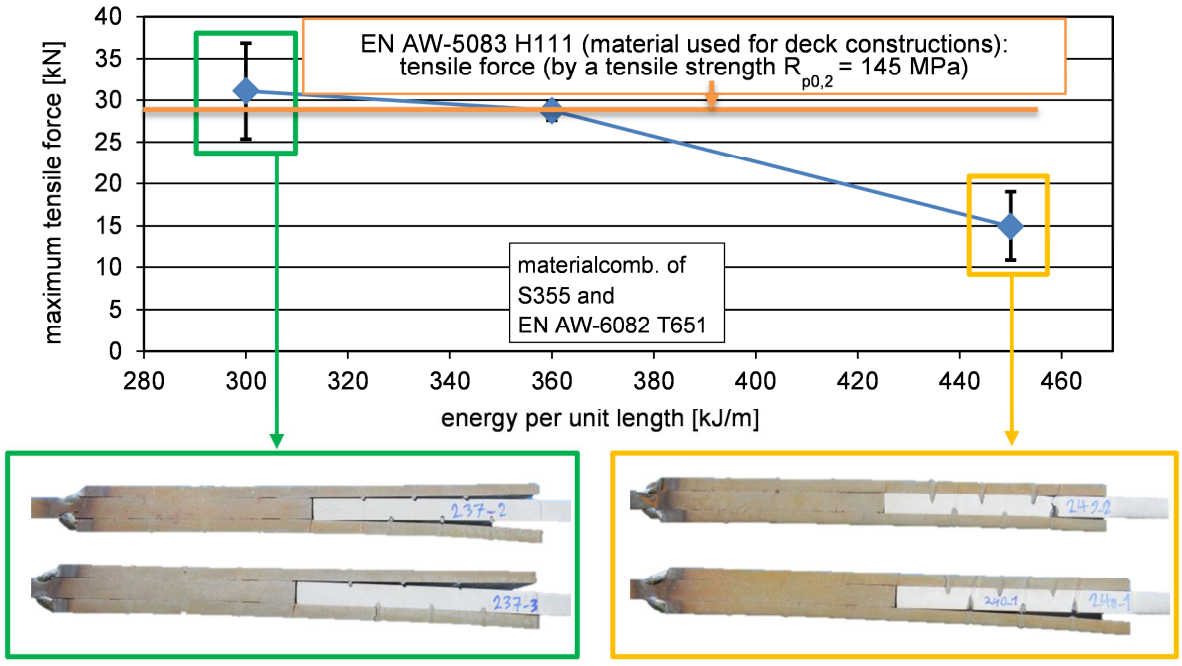

Fig. 7 - Maximum tensile force under quasi-static loading of the adapter consisting of S355 and EN AW-6082 T651, as a function of the energy per unit length; also showing representative different failures types

The maximum tensile force depends on the achieved penetration depth and the weld width, as a result of the defined energy per unit length. Thereby, the average maximum tensile force decreases with increasing energy per unit length. Using an energy per unit length of 300 kJ/m, an average maximum tensile force of 31 kN can be achieved. The base material of the aluminium alloy EN AW-5083 H111 is able to resist a force of 29 kN (for a tensile strength of 145 MPa), which is exceeded by 7 % for the adapter specimen. Due to comparably low penetration depths, such weld seams unbutton under quasi-static loading. The highest

measured tensile force of more than 35 kN was observed for one tensile test in the test series with $E = 300$ kJ/m, which failed by simultaneous unbuttoning of all six weld seams (marked in green in Fig. 7, top). Due to a variation in penetration depth, a one-sided failure can occur and, consequently, the maximum tensile force is reduced to 25 kN (marked in green in Fig. 7, bottom). An increased energy per unit length leads to a reduced tensile force of 15 kN (marked in yellow in Fig. 7).

Evaluation under cyclic loading

For the fatigue assessment, tests under axial cyclic tensile pulsating loading (load ratio of $R = 0$) at constant load amplitude (*Wöhler* tests) were performed on a servohydraulic test rig at a frequency of 30 Hz until total rupture of the specimen. Characteristic parameters concerning the welding process and specimen measurements (mean value) of six test series (TS), which were deemed the most favourable on the basis of the geometrical and quasi-static assessments, are documented in Table 2. The geometrical ratio between weld width and penetration depth has been added to Table 2.

Table 2 - Overview of characteristic parameters of test series for fatigue testing of lap joints with one and three weld seams as well as adapter specimens with six weld seams

Test series (TS)	Number of weld seams	Welding speed v_w [m/min]	Energy per unit E [kJ/m]	Defocusing Δz [mm]	Spot diameter d_s [mm]	Weld width w_w [mm]	Penetration depth d_p [mm]	$\frac{w_w}{d_P}$
1A	1	1.2	300	-12.5	1.63	1.4	2.2	0.6
1B	1	1.0	360	-12.5	1.63	1.6	3.2	0.5
1C	1	1.2	300	-12.5	1.63	1.6	1.4	1.1
3B	3	1.0	360	-12.5	1.63	2.0	2.5	0.8
3C	3	1.2	300	-12.5	1.63	1.7	1.5	1.2
6C	6	1.2	300	-12.5	1.63	1.6	2.2	0.7

The *Wöhler* tests showed a deviating failure behaviour compared with the tensile tests. Furthermore, different modes of failure were observed within the test series for lap joints with one weld seam. These can be explained with the help of camera tracking to the side of the specimens, so that the modes of failure in Fig. 8 were characterised as follows (red arrows denote the loading direction):

a) Failure due to crack propagation through the aluminium base material and crack initiation in the transition from the fusion zone to the aluminium sheet (representative failure of the test series 1A and 1C).

b) Failure due to shear through the weld seam (representative for test series 1B), which can be traced back to cracks within the weld seam. This was confirmed by computer tomographic measurements.

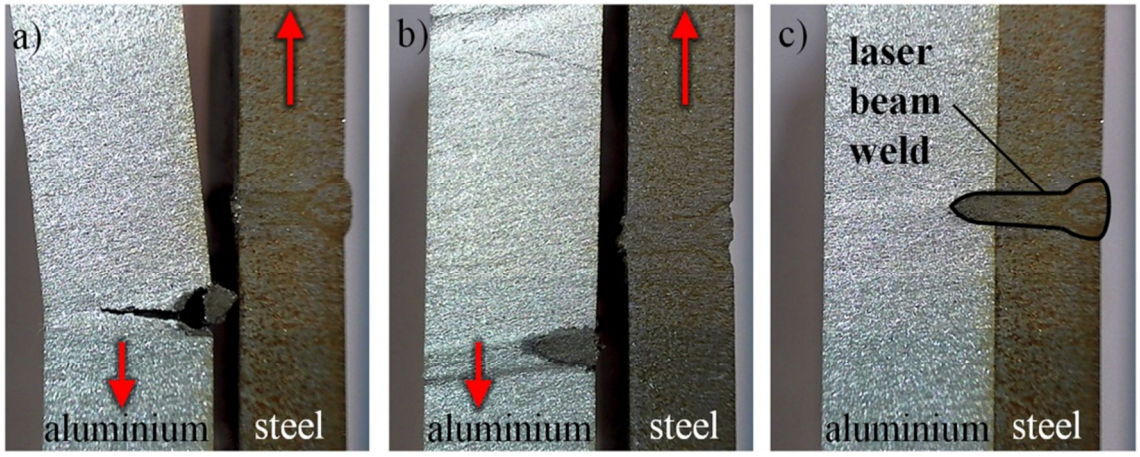

Fig. 8 - Modes of failure in fatigue testing of lap joints with one weld seam (side view) due to crack propagation through the aluminium base material (a) and due to shear through the weld seam (b) compared to the non-load condition (c)

The evaluation of approximately 8 fatigue tests in each test series, according to the Maximum Likelihood Method (Spindel and Haibach, 1978), resulted in load-dependent *Wöhler* curves, as shown in Fig. 9. In addition to the scatter T_F, the *Wöhler* curves were defined by the load amplitude F_a at cycles to failure of $N = 2 \cdot 10^6$, a knee point N_k as well as the slope before (k) and after (k^*) the knee point. The slope after the knee point was set to $k^* = 22$, corresponding to the recommendations for welded joints (Hobbacher, 2016; Sonsino 2007). The *Wöhler* curve for test series 1B, characterised by a width-to-depth ratio of $w_w/d_p = 0.5$ and shear failure, showed the lowest fatigue strength. The fatigue strength increased with rising weld width per penetration depth for TS 1A ($w_w/d_p = 0.6$) and especially for TS 1C ($w_w/d_p = 1.1$), while the scatter was decreased. A high weld width, a reduced penetration depth and a good weld seam quality in terms of a small crack length were the key considerations for increasing the fatigue strength.

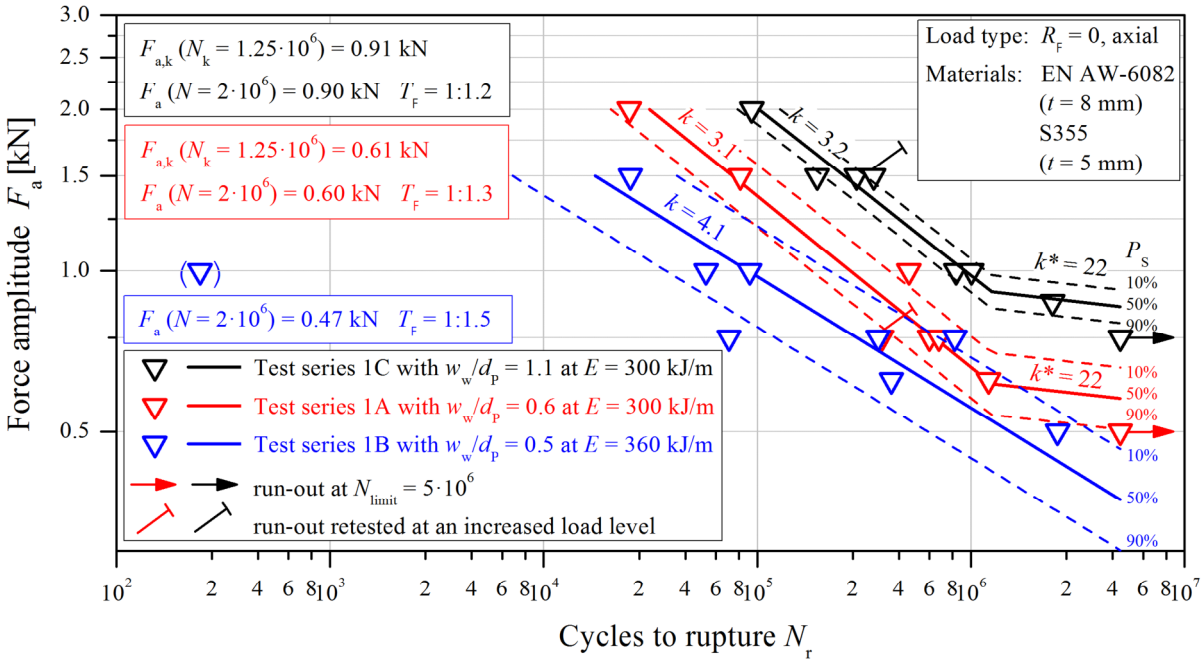

Fig. 9 - *Wöhler* curves for fatigue test results of lap joints with one weld seam

For two different sets of welding process parameters, 11 to 12 fatigue tests ($R = 0$) on lap joints, with triple weld seams (test series 3B and 3C, see Table 2) and a free length of approximately 160 mm, were performed. In another test series on adapter specimens with six weld seams (TS 6C, see Table 2) and a free length of 162 mm, 13 test results were achieved. Crack propagation through the aluminium sheet starting from the tip of the fusion zone, Fig. 8 (a), was identified to be the representative mode of failure for these tests under cyclic loading.

Wöhler curves for lap joints with a triple weld seam and adapter specimens with six weld seams, evaluated according to (Spindel and Haibach, 1978), are compared to that with a triple weld seam in Fig. 10. All slopes of the *Wöhler* curves in the high cycle fatigue regime were almost parallel, within the range $3.1 \leq k \leq 3.4$. Values for the scatter T_F, the fatigue strength in terms of load amplitudes F_a at cycles to failure of $N = 2 \cdot 10^6$ and at the knee point N_k have been added to Fig. 10. For lap joints, *Wöhler* curves of the test series 1C and 3C show increased fatigue strengths compared to TS 1A and 3B and this can be traced back to the influence of the width-to-depth ratio. Finally, an additional increase in fatigue strength to $F_a = (N = 2 \cdot 10^6) = 1.28$ kN was found for adapter specimens.

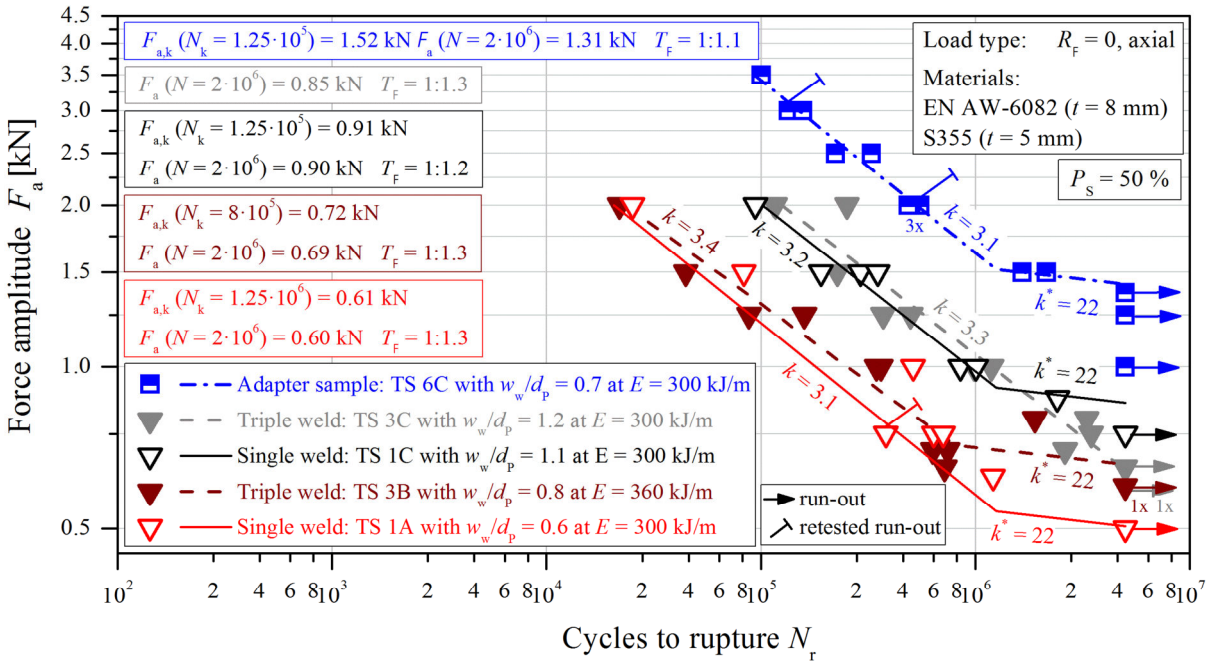

Fig. 10 - *Wöhler* curves for the comparison of lap joints with a single and a triple weld seam as well as adapter specimens with six weld seams

CONCLUSIONS AND OUTLOOK

The feasibility of using a laser beam welding process for steel-aluminium joints was demonstrated at bench scale. The investigation on the welding process parameters included a variation of the focal length and the energy per unit length. On increasing the energy per unit length, the weld width, the penetration depth and, furthermore, the crack length measured from the micro-section all increased. On the basis of quasi-static parameters for steel-aluminium welds, high shear forces were found for the energies per unit length of 300 kJ/m

and 360 kJ/m (corresponding to welding speeds v_w = 1.2 m/min and v_w = 1.0 m/min) using a spot diameter of 1.2 mm. For lap joints with single weld seams, a maximum shear force of 10 kN and, for triple weld seams, a maximum shear force of 21 kN could be achieved (both for E = 300 kJ/m). Realisation of an adapter with six weld seams to join steel and aluminium (double sided each with three welds), resulted in an additional increase in the average maximum tensile force of 31 kN (E = 300 kJ/m).

The comparison of *Wöhler* curves for lap joints with a single and a triple weld seam shows that the influence of the applied welding process parameters and the local weld geometry, i.e. weld width and penetration depth, are the dominating effects for a fatigue assessment, in contrast to the number of weld seams. As a result, from Fig. 11 (a), no increase of the fatigue strength (-6 %) for triple weld seams (TS 3C), compared with single weld seams (TS 1C), was found at an energy per unit length of 300 kJ/m (welding speed v_w = 1.2 m/min). This can be traced back to the fact that the cracks at single and at triple weld seams preferably initiate at one (of the three) welds. Therefore, the weld seams are characterised by the weld width and penetration depth and their ratio. Due to a higher width-to-depth ratio of 1.1 (TS 1C) and 1.2 (TS 3C), these test series showed an increased fatigue strength in comparison to test series with w_w/d_p = 0.5 (TS 1B) and w_w/d_p = 0.8 (TS 3B).

An approximately linear relationship between the averaged width-to-depth ratio and the force amplitude at cycles to failure of $N_f = 2 \cdot 10^6$ can be assumed for fatigue results of lap joints with single and triple weld seams, Fig. 11 (b). An optimisation of the local weld geometry with reference to fatigue properties is conceivable using the width-to-depth ratio.

This finding cannot be transferred directly to the adapter specimens with six weld seams, which show an increase in fatigue strength by a factor of 1.5 to 1.7 compared to lap joints with a high width-to-depth ratio, but themselves are characterised, on the contrary, by w_w/d_p = 0.7. The reason for this observation can be found in the symmetric structure of the adapter, which minimises bending moments of a secondary order. Furthermore, a potential to increase the fatigue strength by optimisation of the weld geometry (high width-to-depth ratio, minimisation of the crack length) of lap joints is derived.

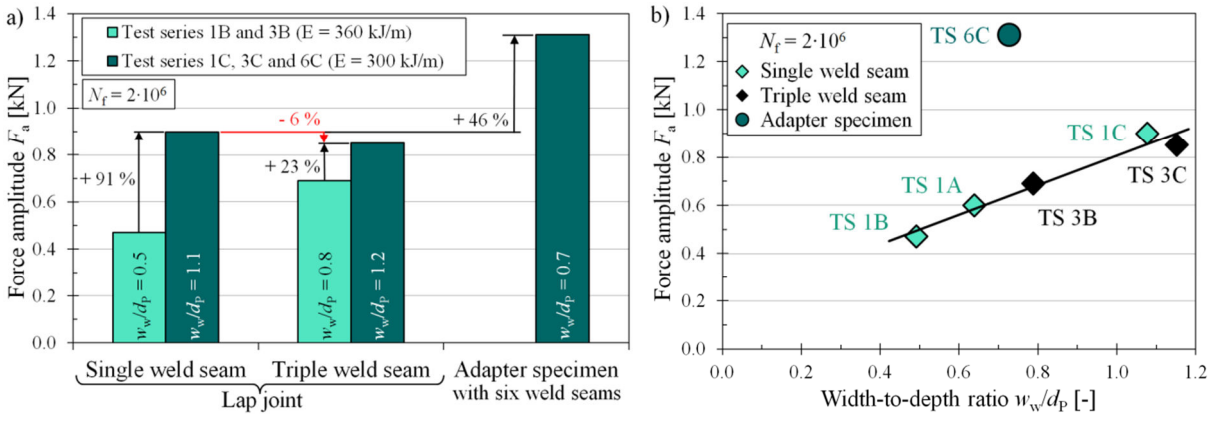

Fig. 11 - Comparison of the fatigue test results of lap joints with a single and a triple weld seam as well as adapter specimens with six weld seams

The evaluation of the influence of weld geometry on quasi-static and cyclic strength confirms the need of a welding process with a precisely adjustable weld shape. For this reason, a laser welding head with an integrated control of the penetration depth will be developed in order to not only realise welding at the bench scale, but also in the industrial field. The optimisation of the welding process parameters is a promising route to strength improvement, under quasi-static as well as cyclic loading. Questions to be answered concern the distribution of stresses at each of the weld seams in joints with multiple welds and the opportunity to improve the load distribution. Steel-aluminium joints should finally be assessed under consideration of ship design recommendations, i.e. guidelines of the DNV-GL, to translate from a load-dependent system to a local fatigue assessment. In this context, the numerical modelling of investigated specimens using the finite element method and the application of the reference radius concept are planned. Additionally, constant and variable amplitude loading that consider environmental impact, such as sea water corrosion, on the fatigue strength of steel-aluminium joints will be investigated.

ACKNOWLEDGMENTS

The joint project “Laser Welding of Steel to Aluminum for Applications in Shipbuilding” (LaSAAS), supervised by the Forschungszentrum Jülich GmbH (PtJ), Zimmerstraße 26-27, 10969 Berlin, has been funded by the German Federal Ministry for Economic Affairs and Energy (BMWi). The authors would like to thank the project partners and the project committee member companies, as well as their representatives, for supporting the project and for their good cooperation.

REFERENCES

[1]-Buijs K. Triplate: The ultimate solution for welding aluminum to steel. HSB International, 2004.

[2]-FSW-Ship project: Rührreibgeschweißte Leichtbaustrukturen für Schiffsaufbauten. Final report, Abeking & Rasmussen Schiff- und Yachtwerft Aktiengesellschaft, 2013.

[3]-Hobbacher A. Recommendations for Fatigue Design of Welded Joints and Components. Springer International Publishing, 2016. doi:10.1007/978-3-319-23757-2

[4]-ICCT - The International Council on Clean Transportation. The Energy Efficiency Design Index (EEDI) for New Ships. Publication of The ICCT, 2011.

[5]-Kallage P. Laserschweißen von Mischverbindungen aus Aluminium und verzinktem sowie unverzinktem Stahl. Dissertation, Gottfried Wilhelm Leibniz Universität Hannover, 2013.

[6]-Klock H, Schroer H. Schweißen und Löten von Aluminiumwerkstoffen. Deutscher Verlag für Schweißtechnik, Düsseldorf, 1977.

[7]-Kreimeyer M, Beckmann M, Wagner F, Vollertsen F. Umformen lasergefügter Fe/Al- und Ti/Al Tailored Hybrid Blanks. 11th Sächsische Fachtagung Umformtechnik (SFU), Freiberg, 2004, p. 343-353.

[8]-Lahdo R, Springer A, Pfeifer R, Kaierle S, Obermeyer L. High-power laser welding of thick steel-aluminum dissimilar joints. Physics Procedia 2016, 83, p. 396-405.

[9]-Sonsino CM. Course of SN-curves especially in the high-cycle fatigue regime with regard to component design and safety. International Journal of Fatigue, 2007, vol. 29, no. 12, pp. 2246-2258.

[10]-Spindel JE, Haibach E. The Method of Maximum Likelihood applied to the Statistical Analysis of Fatigue Data including Run-Outs. S. E. E. International Conference 3 - 6. April 1978, p. 7.1-7.23.